Hindawi
Geofluids
Volume 2022, Article ID 4223791, 14 pages
https://doi.org/10.1155/2022/4223791

Research Article

Study on Durability of Concrete under Alkali-Aggregate Reaction

Mingchang Hei,[1] **A. Fayou**,[2] **Xiong Jia**,[3] **Wenbin Peng**,[2] **and Chuan Yin**[4]

[1]*State Key Laboratory of Hydraulics and Mountain River Engineering, College of Water Resource & Hydropower, Sichuan University, Chengdu, Sichuan 610065, China*
[2]*Faculty of Land Resources Engineering, Kunming University of Science and Technology, Kunming, 650093 Yunnan, China*
[3]*College of Education for the Future, Beijing Normal University, Beijing 100875, China*
[4]*Yunnan Construction and Investment Holding Group Co., Kunming, 650000 Yunnan, China*

Correspondence should be addressed to Mingchang Hei; mingchanghei0816@163.com

Received 29 January 2022; Revised 11 May 2022; Accepted 17 May 2022; Published 9 June 2022

Academic Editor: Xuelong Li

The alkali-aggregate reaction has always had a great impact on the safety and durability of concrete projects. Therefore, the study of concrete failure mechanism under alkali-aggregate reaction has become a hot topic in the engineering field. This paper takes the Longtanqing debris flow ditch concrete treatment project as the background. Based on the alkali-aggregate reaction inhibition test under different conditions, regression analysis and trend surface analysis were used to study the correlation between fly ash content, expansion rate of concrete specimens, and curing age. And the engineering measures are put forward to effectively inhibit the alkali-aggregate reaction: (1) the optimum amount of fly ash appears at 30%-40%, fly ash has the strongest ability to inhibit alkali-aggregate reaction; when the content of fly ash is less than 20%, the fly ash ability to inhibit alkali aggregate reaction is weak. (2) To lower the height of the alkali content of concrete, there is 35% of the grade I class F coal ash as concrete admixture.

1. Introduction

Alkali-aggregate reaction is called the "cancer" of concrete, seriously affecting the safety and durability of concrete engineering [1]. Alkali-aggregate reaction in concrete is as follows: numerous cracks appeared on the surface of the concrete, these cracks usually show "map shape" or "netted," white jelly often flows out of the cracks and gathers and falls off on the crack surface, and jelly can turn into white sediments after air drying [2]. Since the discovery of alkali-aggregate reaction, scholars all over the world have mainly studied the occurrence conditions of alkali-aggregate reaction and the form of damage caused by concrete. Tang proposed using the mixture composed of cement and mineral admixture to inhibit the alkali-aggregate reaction and obtained the hypothesis of "alkalinity balance" [3, 4]. Ramlochan et al. studied the inhibition effect of kaolin on alkali-aggregate raction after kaolin burning [5]. Bektas et al. studied the inhibition mechanism of acidic leva lava to alkali-aggregate reaction [6]. Thomas et al. studied the inhibition mechanism of alkali-aggregate reaction [7]. Zhou and Zhou proposed that the alkali ions in concrete solution is also a key factor affecting the alkali-aggregate reaction [8]. Feng et al. studied the inhibitory effect of aluminum-containing composite materials on alkali-aggregates [9]. Khan studied the inhibition effect of single or compounded mineral admixtures on alkali-aggregate reaction of high-performance concrete. It is concluded that the expansion rate of concrete is low and has better inhibition effect [10]. Harbec et al. compared the difference in durability between high-performance concrete mixed with glass fume (GF) and high-performance concrete mixed with silica fume (SF) [11]. Xu et al. put forward that the key to solve the problem of alkali-aggregate reaction lies in how to correctly judge the existence of alkali activity of aggregate [12]. Liu proposed a draft method for evaluating the effectiveness of fly ash in inhibiting ASR in practical engineering concrete [13]. Salim and Mosaberpanah provide a comprehensive review on the

mechanism, causes of AAR, and the behavior/performance of different geopolymers (a combination of an alkaline liquid with fly ash, metakaolin, and blast furnace slag) and mineral admixtures (fly ash, highly reactive metakaolin) when used to eliminate AAR and their effect on different mechanical properties of concrete [14]. Zhuang et al. discuss the factors affecting the performances of fly ash-based geopolymer concrete [15]. Hemalatha analysis structure-property of fly ash reported in various literature and its correlation with strength and durability characteristics [16]. Pertinent to the optimal and broad utilization of fly ash as an integral part of sustainable construction materials, Xu and Shi identify for further research and development [17]. The discussion concludes that geopolymers and mineral admixtures work efficiently in the mitigation of AAR if they are used in an appropriate percentage; they not only reduce/mitigate AAR but also significantly increase the mechanical properties of concrete [14].

It can be seen from the above research that the research on the inhibition of the alkali-aggregate reaction mainly focused on the research on the inhibitory effect of a single mineral admixture or multiple mineral admixtures [18–22]. There are few studies on using fly ash as admixture to inhibit alkali aggregate reaction. Fly ash is one of the largest industrial waste residues in the world. Fly ash can be used as a resource. It has been widely promoted as an admixture for concrete. The mechanism of fly ash on the alkali-aggregate reaction of concrete dams has been studied. The inhibitory effect can not only optimize concrete alkali-aggregate reaction inhibitory measures but also increase the degree of resource utilization of fly ash, which has certain theoretical and practical significance.

2. Selection and Text Methods of Raw Materials

2.1. Raw Materials. According to the conditions of alkali-aggregate reaction, sand and stone produced by a quarry in Huaning County, Yuxi city, Yunnan province, are selected as aggregates (refer to "Specifications of mineral exploration for aggregate rock materials DZ-T 0341-2020" and "Technical code for prevention of alkali-aggregate reaction in concrete GB/T 50733-2011") [23]. After the rapid identification of the mortar rod, the expansion rate of 14 days was 0.34%, which proved that the aggregate was the active aggregate. The P.S.A32.5 and P.O42.5 cement produced by Huaning Yuzhu Cement Factory were selected as the gel material. The main physical properties of cement are shown in Table 1, and the chemical composition is mainly silica (SiO_2), aluminium oxide (Al_2O_3), magnesium oxide (MgO), sodium oxide (Na_2O), potassium oxide (K_2O), etc.

The suppression method of alkali-aggregate reaction was studied, and Xuanwei Grade I coal ash was selected as the inhibitory material. The coal ash used in the experimental is class I class F coal ash produced by a power plant in Xuanwei. The fineness is 7.4 (standard: 45 μm square hole sieve ≤12%), and the burning loss is 3.3% (standard: ≤5%). The chemical composition of coal ash is shown in Table 2.

2.2. Preparation and Maintenance of Specimen. Main equipment: alkali-aggregate reaction maintenance box (Figure 1), length measuring instrument press (Figure 2) and mold, maintenance barrel, and oven.

First, the aggregate is made into a sand sample and reduced to about 5 kg. Make up the experimental materials according to the grading and scale mix shown in Table 3 and use the dryer to drying the standby. The quality ratio of cement to sand according to 1 : 2.25, and the water-ash ratio according to 0.47 to take the materials required for the experimental piece. In order to study the inhibition effect of coal ash on alkali-aggregate reaction, replace cement with 0%, 20%, 30%, 35%, and 40% equivalent substitute coal ash, and prepare the mortar rod specimen according to the proportioning shown in Table 4. Each proportioning production is a set of specimen, each set of specimen is 3 specimens. After the specimen is molded, remove the excess mortar with a trowel, smooth the surface of the specimen, and indicate the direction and marking of the measurement. After the specimen has been thoroughly molded, the experimental piece should be molded into the alkali-aggregate reaction maintenance box, demoulding after 24 hours of maintenance.

2.3. Expansion Rate Experimental Step. After the specimen is stripping mold, the specimen should be soaked in a maintenance barrel filled with pure water, note that a maintenance barrel can only hold specimen of the same aggregate, then the maintenance barrel into the alkali-aggregate reaction maintenance box 24 h, to maintain a temperature of 80 degrees C. After 24 h, remove the maintenance barrel one by one at an ambient temperature of 20 degrees C and then remove the experimental piece from the maintenance barrel in turn. The removed specimen is measured with a metroscope as soon as it is wiped clean with a dry towel. The measurement is the base length (L_0) of the specimen. In order to ensure the accuracy of the experimental data, the average value (accurate to 0.02 mm) needs to be measured several times. When measuring, be careful that the completion of the specimen from the time the specimen is removed to the completion of the reading is between 15 and 20 seconds, after the reading with a wet towel to cover the experimental piece in a timely manner. After all the experimental piece measurements are completed, the experimental piece is immersed in a maintenance barrel with a concentration of 1 mol/L of alkali solution, and the maintenance barrel is placed in the alkali-aggregate reaction maintenance box and maintains a temperature of 80 degrees C. On the date of determining the benchmark specimen length (L_0), the length (L_t) shall be measured and recorded on the third day, seven days, ten days, fourteen days, and twenty-eight days, respectively. After the measurement is complete, the experimental piece should be turned around and put into the primary alkali solution for continued maintenance. The expansion rate is calculated as follows:

$$\varepsilon_t = \frac{L_t - L_0}{L_0 - 2\triangle} \times 100. \quad (1)$$

Table 1: The main physical properties of cement table.

Cement		Setting time (min)		Compressive strength (MPa)		Flexural strength (MPa)		Finely
		Initial setting	Final set	3 d	28 d	3 d	28 d	Sieve
P.S.A32.5	Measured value	169	471	13.0	39.9	3.4	7.0	6
	Standard values	≥45	≤600	10.0	32.5	2.5	5.5	≤10
P.O42.5	Measured value	148	335	22.6	49.4	4.6	8.0	3
	Standard values	≥45	≤600	17.0	46.5	3.5	6.5	≤10

Table 2: Main chemical composition of coal ash.

Chemical composition	SiO_2	Al_2O_3	Na_2O	K_2O	MgO	Fe_2O_3	CaO	Total
Coal ash	48.06	34.53	0.44	0.81	0.77	3.75	5.90	94.26

Figure 1: Alkali aggregate reaction curing box.

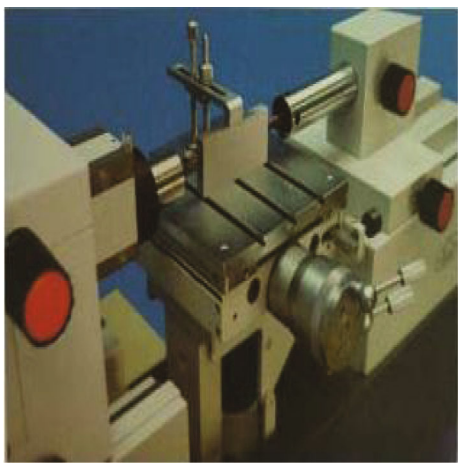

Figure 2: Length measuring instrument.

In the formula, ε_t is the expansion rate of the experimental piece during the t-day age period (%); L_t is the length of the experimental piece in t-day age (mm); L_0 is the benchmark specimen length (mm); and $\triangle$ is the probe length (mm).

3. Analysis of Experimental Results

3.1. Analysis of the Expansion Rate and Results of the Benchmark Experimental Piece. Follow the experimental steps in the previous chapter, and the results are shown in Table 5.

The without dosage of admixture specimen FA-1-0, FA-2-0, FA-3-0, FA-4-0, and FA-5-0 (which are maintained in an 80 degrees C, 1 mol/L alkali solution) will be set as benchmark specimen. By measuring the expansion length of the benchmark specimen and calculating its expansion rate, we can judge the activity of the aggregate, namely, whether an alkali-aggregate reaction has occurred. In order to prove the existence of alkali-aggregate reaction, the comparison experimental J_1, J_2, J_3, J_4, and J_5 and the benchmark experimental piece FA-1-0, FA-2-0, FA-3-0, FA-4-0, and FA-5-0 were also designed in the experiment for comparison one by one. The expansion rate of two sets of specimen in 3 d, 7 d, 14 d, and 28 d was measured and calculated. The results are shown in Figures 3–8.

The expansion rates of the benchmark specimen FA-1-0, FA-2-0, FA-3-0, FA-4-0, and FA-5-0 increase with age. According to the judgment standard of "Code for experimentaling aggregates of hydraulic concrete DLT5151-2014," the average 14-day expansion rate of the five benchmark specimen was greater than 0.2%. The judgment in the previous section was verified—the aggregate is an active aggregate. From the analysis of Figures 3–8, it can be seen that the expansion rate of concrete specimen increases with the continuous pass of maintenance time, and the curve is convex, indicating that the slope of the curve is decreasing, that is, the expansion rate of the preconcrete period is relatively faster compared to the later stage, without dosage of admixture specimens J_1, J_2, J_3, J_4, and J_5 cured in 80°C tap water having the same material composition as the without dosage of admixture specimens FA-1-0, FA-2-0, FA-3-0, FA-4-0, and FA-5-0 cured in 80°C 1 mol/L alkali solution, but the curing conditions are different: the specimens J_1, J_2, J_3, J_4, and J_5 were soaked in tap water at 80 degrees C, and the specimens FA-1-0, FA-2-0, FA-3-0, FA-4-0, and FA-5-0 were soaked in an alkaline solution at 80 degrees C. Specimens J1, J2, J3, J4, and J5 do not expand, while specimens

Table 3: Sand grade table.

Nominal size	2.50 mm~5.00 mm	1.25 mm~2.50 mm	630 μm~1.25 mm	315 μm~630 μm	160 μm~315 μm
Grading quality (%)	10	25	25	25	15

Table 4: The mating ratio of the mortar bar specimen.

The specimen number	Cement alkali content (%)	Cement/g	Replace the amount of cement/g	Dosage of admixture/g
J_1	0.60	440	0	0
FA-1-0	0.60	440	0	0
FA-1-20	0.60	352	20	88
FA-1-30	0.60	308	30	132
FA-1-35	0.60	286	35	154
FA-1-40	0.60	264	40	176
J_2	0.90	440	0	0
FA-2-0	0.90	440	0	0
FA-2-20	0.90	352	20	88
FA-2-30	0.90	308	30	132
FA-2-35	0.90	286	35	154
FA-2-40	0.90	264	40	176
J_3	1.25	440	0	0
FA-3-0	1.25	440	0	0
FA-3-20	1.25	352	20	88
FA-3-30	1.25	308	30	132
FA-3-35	1.25	286	35	154
FA-3-40	1.25	264	40	176
J_4	1.5	440	0	0
FA-4-0	1.5	440	0	0
FA-4-20	1.5	352	20	88
FA-4-30	1.5	308	30	132
FA-4-35	1.5	286	35	154
FA-4-40	1.5	264	40	176
J_5	2.0	440	0	0
FA-5-0	2.0	440	0	0
FA-5-20	2.0	352	20	88
FA-5-30	2.0	308	30	132
FA-5-35	2.0	286	35	154
FA-5-40	2.0	264	40	176

Note: J_1 represents the water maintenance of without dosage of admixture specimen with a base content of 0.60 in water at 80 degrees C; J_2 represents the water maintenance of without dosage of admixture specimen with a base content of 0.90 in water at 80 degrees C; the FA-1-0 experimental piece with a base content of 0.60 without dosage of admixture maintained in an alkali solution of 80 degrees C 1 mol/L; the FA-2-0 experimental piece with a base content of 0.90 without dosage of admixture maintained in an alkali solution of 80 degrees C 1 mol/L; the FA-1-20 experimental piece with a base content of 0.60, and the amount of dosage of admixture is 20% without dosage of admixture maintained in an alkali solution of 80 degrees C 1 mol/L; other specimen numbers are similar to the above.

FA-1-0, FA-2-0, FA-3-0, FA-4-0, and FA-5-0 when soaked to produce a larger expansion indicate that the expansion of reference specimens FA-1-0, FA-2-0, FA-3-0, FA-4-0, and FA5-0 is caused by alkali in the curing environment, the destruction of alkali-aggregate reaction.

3.2. Expansion Rate and Result Analysis of Specimens Mixed with Coal Ash. In order to study the inhibition effect of coal ash on alkali-aggregate reaction, the mortar rod fast method is used to break the aggregate into a fine aggregate with the prescribed grade distribution and proportional combination mixed with gel material (cement, coal ash) to make mortar rod experimental pieces, coal ash inhibition alkali-aggregate reaction effect experimental. The results of the experiment are shown in Figures 9–13.

The results show that:

(1) As can be seen from Table 5 and Figures 9–13, the concrete specimens mixed with coal ash are compared to the benchmark experimental pieces (FA-1-

Table 5: Experimental results.

Experimental piece number	Expansion rate of experimental piece (%)				Expansion reduction rate (%)	
	3 d	7 d	14 d	28 d	14 d	28 d
J_1	0.012	0.015	0.015	0.015	0	0
FA-1-0	0.039	0.078	0.221	0.434	0	0
FA-1-20	0.015	0.018	0.035	0.062	84	85
FA-1-30	0.008	0.012	0.024	0.039	89	91
FA-1-35	0.007	0.010	0.013	0.013	94	97
FA-1-40	0.009	0.013	0.015	0.018	93	95
J_2	0.012	0.014	0.014	0.014	0	0
FA-2-0	0.043	0.113	0.246	0.461	0	0
FA-2-20	0.008	0.027	0.049	0.106	80	77
FA-2-30	0.005	0.016	0.021	0.048	91	89
FA-2-35	0.002	0.015	0.019	0.038	92	91
FA-2-40	0	0.014	0.019	0.037	92	92
J_3	0.013	0.014	0.014	0.014	0	0
FA-3-0	0.044	0.110	0.216	0.408	0	0
FA-3-20	0.008	0.009	0.040	0.109	81	73
FA-3-30	0.007	0.007	0.019	0.031	91	92
FA-3-35	0.016	0.016	0.018	0.030	92	93
FA-3-40	0.017	0.018	0.018	0.029	92	93
J_4	0.012	0.012	0.013	0.013	0	0
FA-4-0	0.052	0.114	0.236	0.418	0	0
FA-4-20	0.008	0.033	0.061	0.102	75	76
FA-4-30	0.005	0.009	0.047	0.081	80	80
FA-4-35	0.004	0.005	0.026	0.051	89	88
FA-4-40	0.004	0.004	0.031	0.054	86	87
J_5	0.014	0.014	0.014	0.015	0	0
FA-5-0	0.059	0.137	0.251	0.470	0	0
FA-5-20	0.018	0.035	0.071	0.116	69	75
FA-5-30	0.005	0.017	0.053	0.085	76	81
FA-5-35	0.004	0.012	0.036	0.069	84	85
FA-5-40	0.005	0.015	0.048	0.072	79	85

0, FA-2-0, FA-3-0, FA-4-0, and FA-5-0); expansion rate is much smaller, usually more than 70%; the more doped, the smaller the expansion rate, indicating that coal ash can effectively inhibit alkali-aggregate reaction to concrete damage

(2) When not mixed with coal ash, the change of cement alkali content has less effect on the expansion rate of concrete experimental pieces, and when the amount of coal ash is ≥20%, the expansion rate of concrete increases with the increase of cement alkali content

(3) When the cement alkali content is certain, the expansion rate of alkali-aggregate reaction experimental piece is negatively correlated with the content of coal ash. When the amount of coal ash doped ≥20%, the expansion rate of 14 d of the alkali-aggregate reaction experimental piece was less than 0.1%. 28 d alkali-aggregate reaction experimental part expansion rate is less than 0.15%, 14 d experimental piece expansion reduction rate is greater than 70%, and 28 d experimental piece expansion reduction rate is also more than 70%, indicating that the powder coal ash inhibition effect is good

3.3. Data Fitting. Four-dimensional surface fitting is carried out on the factors affecting the expansion rate of alkali-aggregate reaction experimental pieces, the maintenance time (age/d) of the experimental piece is used as variable x, the amount of coal ash doped as variable y, and the expansion rate of the experimental piece as the dependent variable z; thus, the function $z - F(x, y)$ is obtained, after programming the data in Table 5 and entering them into the MATLAB software, then perform polynomial surface fitting; the results are as follows.

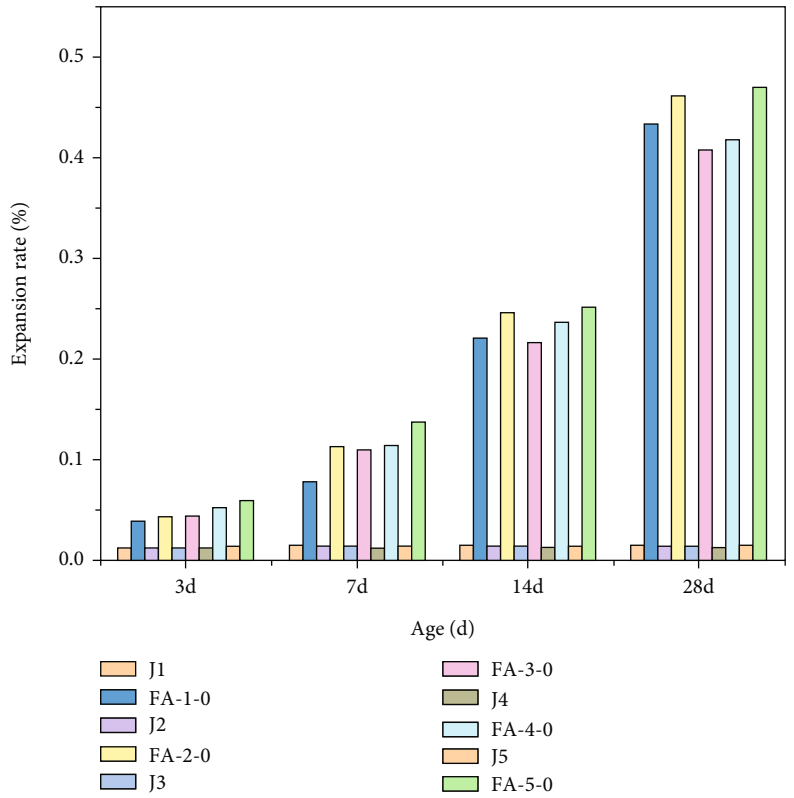

Figure 3: A graph of the expansion rate and age of the reference specimen.

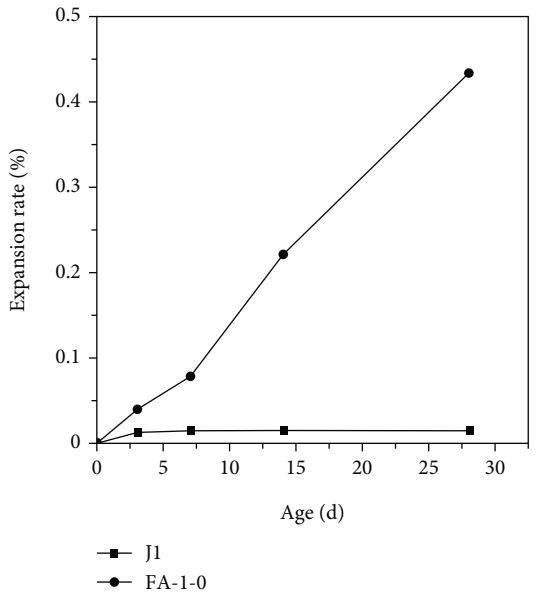

Figure 4: The diagram between FA-1-0 benchmark specimen and age.

Perform trend surface analysis on the fly ash content (x_1), curing days (y_1), and specimen expansion rate (z_1) corresponding to a cement alkali content of 2.00% and obtain the regression equation $z_1 = F(x_1, y_1)$. The quartic regression equation is as follows:

$$\begin{aligned} z_1 = F(x_1, y_1) = {} & p_{00} + p_{10}x_1 + p_{01}y_1 + p_{20}{x_1}^2 \\ & + p_{11}x_1y_1 + p_{02}{y_1}^2 + p_{30}{x_1}^3 + p_{21}{x_1}^2y_1 \\ & + p_{12}x_1{y_1}^2 + p_{03}{y_1}^3 + p_{31}{x_1}^3y_1 \\ & + p_{22}{x_1}^2{y_1}^2 + p_{13}x_1{y_1}^3 + p_{04}{y_1}^4. \end{aligned} \tag{2}$$

The coefficients in the equation $z_1 = F(x_1, y_1)$ are $p_{00} = 0.01021$, $p_{10} = 0.01568$, $p_{01} = -1.088$, $p_{20} = 0.0001907$, $p_{11} = -0.1304$, $p_{02} = 12.29$, $p_{30} = -5.869e-6$, $p_{21} = 0.00076$, $p_{12} = 0.3662$, $p_{03} = -44.24$, $p_{31} = -1.468e-5$, $p_{22} = -0.0002097$, $p_{13} = -0.3675$, $p_{04} = 50.68$.

Perform trend surface analysis on the fly ash content (x_2), curing days (y_2), and specimen expansion rate (z_2) corresponding to a cement alkali content of 1.50% and obtain the regression equation $z_1 = F(x_2, y_2)$. The quartic regression equation is as follows:

$$\begin{aligned} z_2 = \mathrm{F}(x_2, y_2) = {} & \mathrm{p}_{00} + \mathrm{p}_{10}x_2 + \mathrm{p}_{01}\mathrm{y}_2 + \mathrm{p}_{20}{x_2}^2 \\ & + \mathrm{p}_{11}x_2\mathrm{y}_2 + \mathrm{p}_{02}{\mathrm{y}_2}^2 + \mathrm{p}_{30}{x_2}^3 + \mathrm{p}_{21}{x_2}^2\mathrm{y}_2 \\ & + \mathrm{p}_{12}x_2{\mathrm{y}_2}^2 + \mathrm{p}_{03}{\mathrm{y}_2}^3 + \mathrm{p}_{31}{x_2}^3\mathrm{y}_2 + \mathrm{p}_{22}{x_2}^2{\mathrm{y}_2}^2 \\ & + \mathrm{p}_{13}x_2{\mathrm{y}_2}^3 + \mathrm{p}_{04}{\mathrm{y}_2}^4. \end{aligned} \tag{3}$$

The coefficients in the function $z_2 = F(x_2, \mathrm{y}_2)$ are $p_{00} = 0.004306$, $p_{10} = 0.01479$, $p_{01} = -1.706$, $p_{20} = 0.0002397$, $p_{11} = -0.1243$, $p_{02} = 18.48$, $p_{30} = -8.577e-6$, $p_{21} = 0.001019$, $p_{12} = 0.3262$, $p_{03} = -63.51$, $p_{31} = -1.504e-5$, $p_{22} = -4.354e-5$, $p_{13} = -0.3507$, $p_{04} = 70.39$.

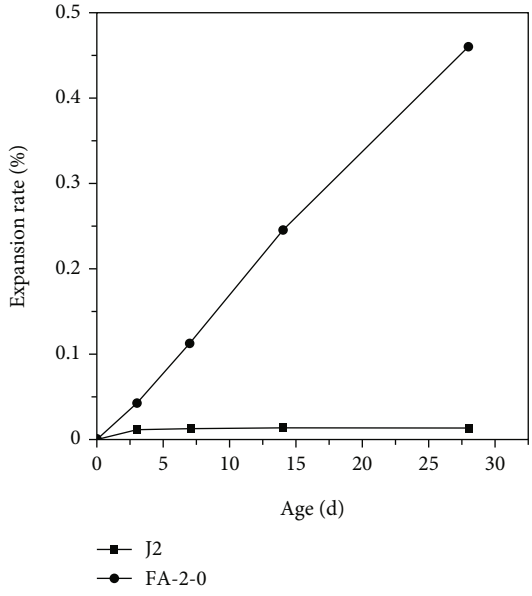

Figure 5: The diagram between FA-2-0 benchmark specimen and age.

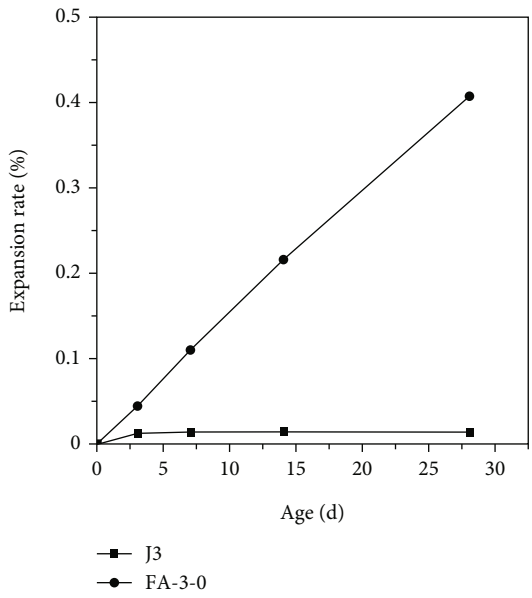

Figure 6: The diagram between FA-3-0 benchmark specimen and age.

Perform trend surface analysis on the fly ash content (x_3), curing days (y_3), and specimen expansion rate (z_3) corresponding to a cement alkali content of 0.90% and obtain the regression equation $z_3 = F(x_3, y_3)$. The quartic regression equation is as follows:

$$\begin{aligned} z_3 = \mathrm{F}(x_3, y_3) &= \mathrm{p}_{00} + \mathrm{p}_{10}x_3 + \mathrm{p}_{01}y_3 + \mathrm{p}_{20}{x_3}^2 \\ &+ \mathrm{p}_{11}x_3y_3 + \mathrm{p}_{02}{y_3}^2 + \mathrm{p}_{30}{x_3}^3 + \mathrm{p}_{21}{x_3}^2y_3 \\ &+ \mathrm{p}_{12}x_3{y_3}^2 + \mathrm{p}_{03}{y_3}^3 + \mathrm{p}_{31}{x_3}^3y_3 + \mathrm{p}_{22}{x_3}^2{y_3}^2 \\ &+ \mathrm{p}_{13}x_3{y_3}^3 + \mathrm{p}_{04}{y_3}^4. \end{aligned} \quad (4)$$

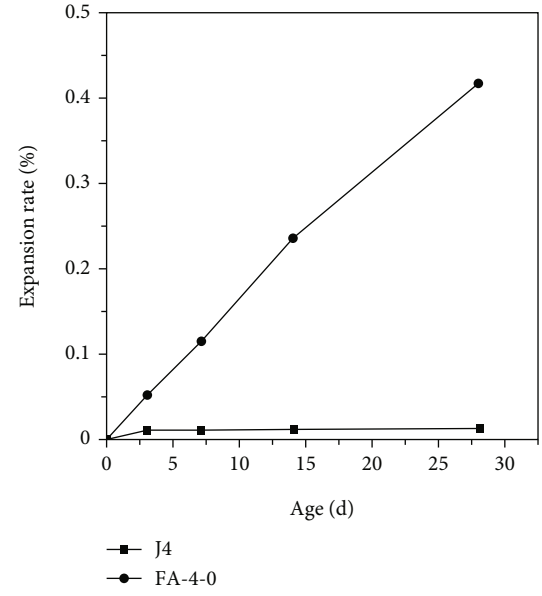

Figure 7: The diagram between FA-4-0 benchmark specimen and age.

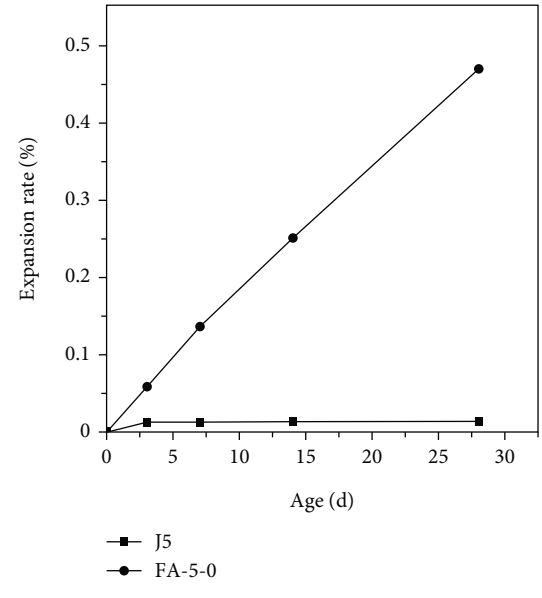

Figure 8: The diagram between FA-5-0 benchmark specimen and age.

The coefficients in the equation $z_3 = F(x_3, y_3)$ are $p_{00} = -0.006757$, $p_{10} = 0.01557$, $p_{01} = 0.004563$, $p_{20} = 0.000308$, $p_{11} = -0.1013$, $p_{02} = 0.1179$, $p_{30} = -9.547e-6$, $p_{21} = -0.001652$, $p_{12} = 0.2621$, $p_{03} = -0.3238$, $p_{31} = 6.01e-5$, $p_{22} = -0.001997$, $p_{13} = -0.1144$, $p_{04} = -0.6845$.

As can be seen from above, coal ash doping and maintenance period (age) can affect the expansion rate of concrete, and then, according to Figures 14–16, adding coal ash concrete expansion rate over time changes and specific values. From this, we can deduce the change and specific numerical of concrete expansion rate with time after adding coal ash when the alkali content of cement is certain. From the above

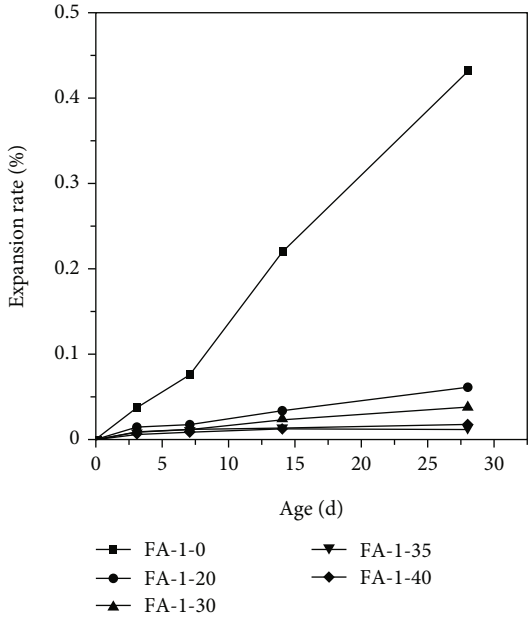

Figure 9: Graph of the expansion rate of the specimen and the amount of coal ash content (cement alkali content 0.60%).

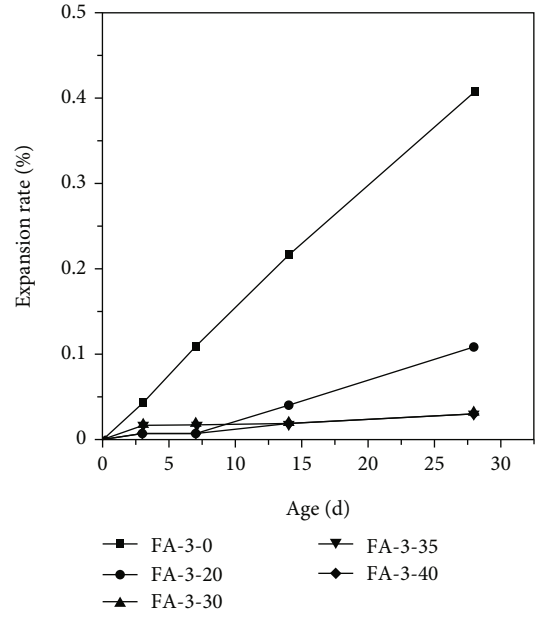

Figure 11: Graph of the expansion rate of the specimen and the amount of coal ash content (cement alkali content 1.25%).

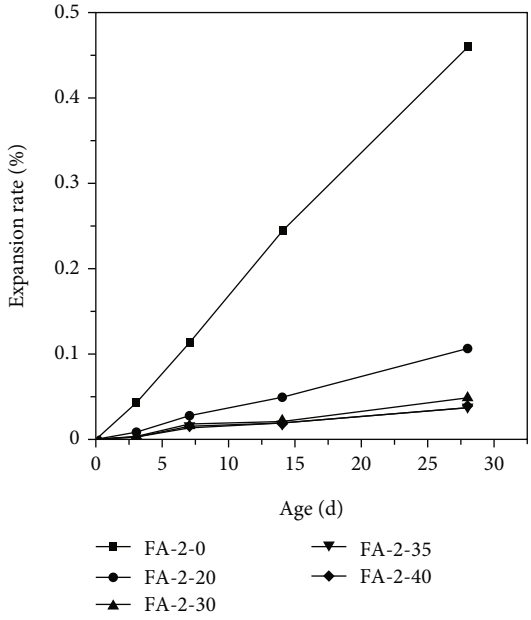

Figure 10: Graph of the expansion rate of the specimen and the amount of coal ash content (cement alkali content 0.90%).

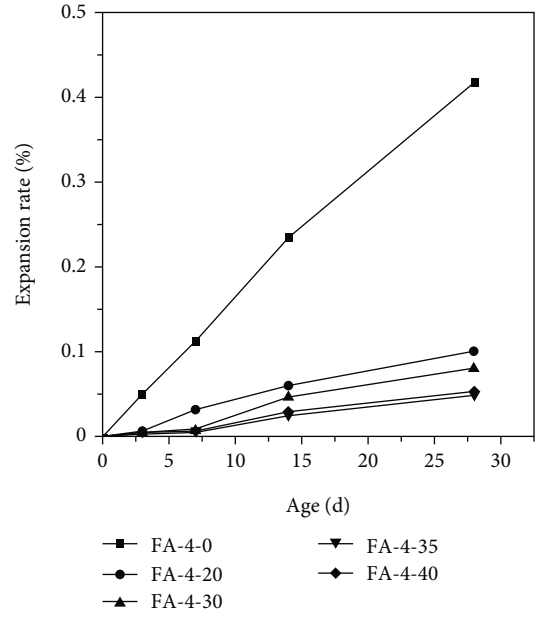

Figure 12: Graph of the expansion rate of the specimen and the amount of coal ash content (cement alkali content 1.50%).

fitted surface, it can be seen that the expansion rate of concrete alkali-aggregate reaction shows: when the amount of coal ash doping is not less than 30% under high alkali conditions, it can effectively inhibit the alkali-aggregate reaction; the greater the amount of coal ash doping, the stronger the inhibition effect. The optimum point of coal ash shows doping 30% to 40%; the expansion rate of concrete experimental pieces under the doping is least affected by the maintenance age; when the ash content of coal ash is less than 20%, the expansion rate of concrete experimental pieces increases with the increase of maintenance age, and the growth rate accelerated when the age period reached 14 days, indicating that the inhibition ability of low-doped coal ash to alkali-aggregate reaction was weak. The above two points show that the amount of coal ash mixed in concrete should be greater than 20%, but considering the performance of concrete, the amount of coal ash in concrete should not exceed 40%; otherwise, it will easily cause concrete bleeding phenomenon, affecting the strength and durability of concrete.

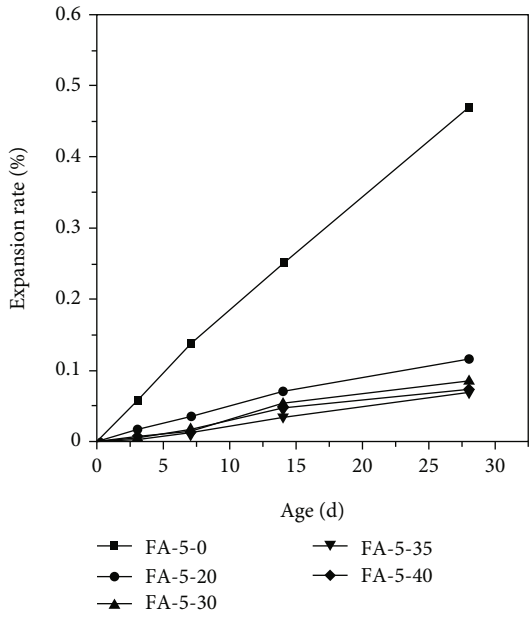

Figure 13: Graph of the expansion rate of the specimen and the amount of coal ash content (cement alkali content 2.00%).

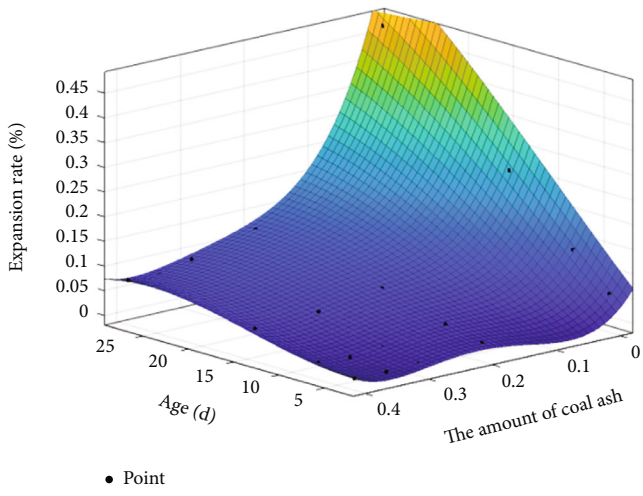

Figure 14: Quartic fitting diagram of coal ash content, age, and expansion rate (cement alkali content 2.0%).

3.4. Analysis of Inhibition Mechanism of Coal Ash on Alkali-Aggregate Reaction. To solve the destructive expansion of alkali-aggregate reaction to concrete, we can start with the mechanism of the reaction itself. Such as alkali-silica acid reaction, the reaction is the reaction between amorphous form silica and hydrated silica in the aggregate and the alkaline ions in the concrete pore solution on the surface of silica particles and releases chemical energy when the reaction occurs. Silicon dioxide particles in the reaction can be thought of as a small energy center, which breaks the relatively balanced energy in the concrete hole solution, brings the dispersed energy in some areas to the center, resulting in a certain point inside the concrete that is too powerful, and when that energy is strong enough to break a certain

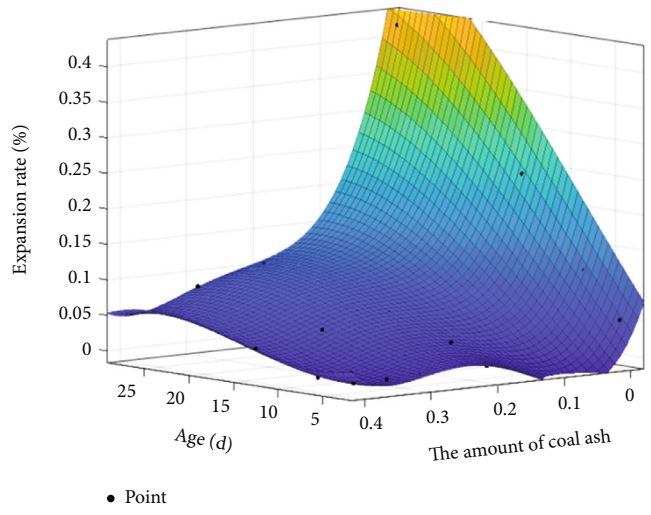

Figure 15: Quartic fitting diagram of coal ash content, age, and expansion rate (cement alkali content 1.50%).

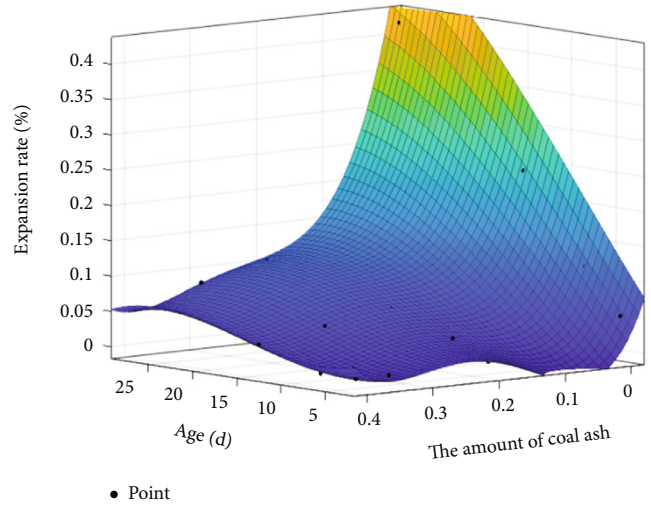

Figure 16: Quartic fitting diagram of coal ash content, age, and expansion rate (cement alkali content 0.90%).

limit, it will destroy the concrete structure locally, resulting in local cracks in the concrete. From this analysis, if the locally increased expansion force (energy) is dispersed to the whole (an area), that is, there is an infinite number of energy centers in an area, the energy originally gathered to a point is dispersed to this infinite number of centers, it will certainly not make a specific point of energy exceed the limit, and thus can be very good inhibition of alkali-aggregate reaction. The coal ash mixed with concrete contains a large number of active silica particles, each of which can act as an energy center or reaction center. Because the silica particles in coal ash are extremely small, so when a certain amount of coal ash is mixed into the concrete, the coal ash will be evenly distributed in various parts of the concrete, forming a large number of energy centers or reaction

centers. When the alkali content of concrete is certain, the increase of energy center or reaction center means that the originally locally accumulated expansion force is dispersed to the whole, which is a process from point to surface and then to the body. The increased energy center or reaction center disperses the energy, result in cannot concentrate it, dissolves the destruction of the concrete structure of the energy, and effectively inhibits the alkali-aggregate reaction [17, 24].

Coal ash, also known as coal ash, is a fine particle powder consisting mainly of spherical glass particles produced during the combustion of coal ash. After a strong quenching process formed, a relatively dense undercooling glass structure, especially the surface layer is very tight, it is necessary to go through the action of hydroxyl ions to show activity. For coal ash, after activation, a large number of glassy particles in coal ash will dissolve and collapse, increase the surface area, produce a large number of silicon hydroxyloh and Al-OH groups, quickly adsorb a large number of alkali metal ions in concrete, and consume a large number of hydroxyl ions, so as to reduce the pH value of concrete and further inhibit the alkali-aggregate reaction.

The inhibition of alkali-aggregate reaction by coal ash first shows the consumption of alkali solution of concrete by coal ash, including alkali metal ions and hydroxyl ions in the solution. Since there is a certain amount of active inhibitory components in coal ash, when the consumption of alkali reaches a considerable degree, the consumption of alkali will be replaced by the consumption of calcium. When the calcium ion concentration inside the concrete increases, it will replace the position of alkaline cations, replace part of the alkali from the adsorption state of coal ash, and repeat the above process for the unactivated active glass again until all the active inhibitory components are reacted. The final products are calcium silicate, hydrate of calcium aluminate, and silica alumina gel [25].

In the use of concrete with a high content alkali amount, coal ash can only reduce the alkali concentration in the concrete hole solution in a short period of time, and then, calcium adsorption becomes an advantage; alkali-aggregate reaction will keep going. The effect of coal ash on the initial stage of inhibiting alkali-aggregate reaction is mainly to significantly reduce the alkali concentration in the solution inside concrete and to greatly reduce the reaction strength in the initial stage of alkali-aggregate reaction. According to the basic viewpoint of "catastrophe theory" (or catastrophe theory), the expansion cracking of concrete is nonlinear, uncertain, and discontinuous. Before the concrete breaks ("transition"), if the penetration, diffusion, and convergence rate of reaction substances and the accumulation rate of reaction products in alkali-aggregate reaction are strictly controlled to slow down, then the catastrophe (catastrophe) stage is stable, the explosion of generated energy will tend to ease, and the destructive capacity will be greatly reduced; the alkali-aggregate reaction becomes a gradual process. If the "alkaline equilibrium" hypothesis is followed, active components such as silica in coal ash are considered acidic. Then, the higher the active acid oxide content in coal ash, the less alkaline oxide, the better the inhibition effect of coal ash.

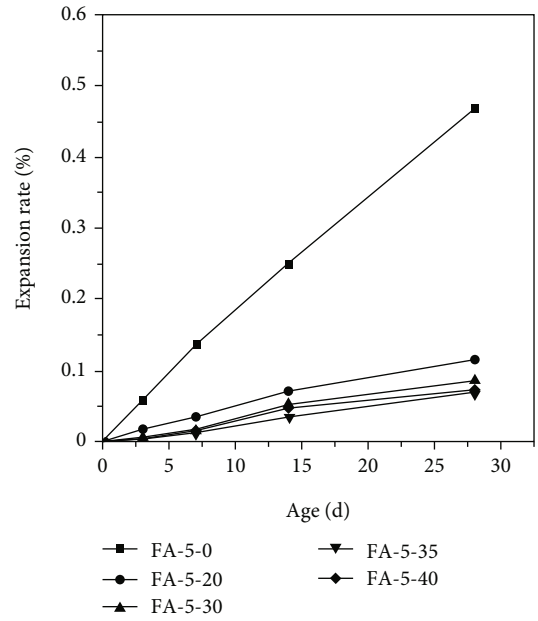

Figure 17: Effect of coal ash on alkali-aggregate reaction.

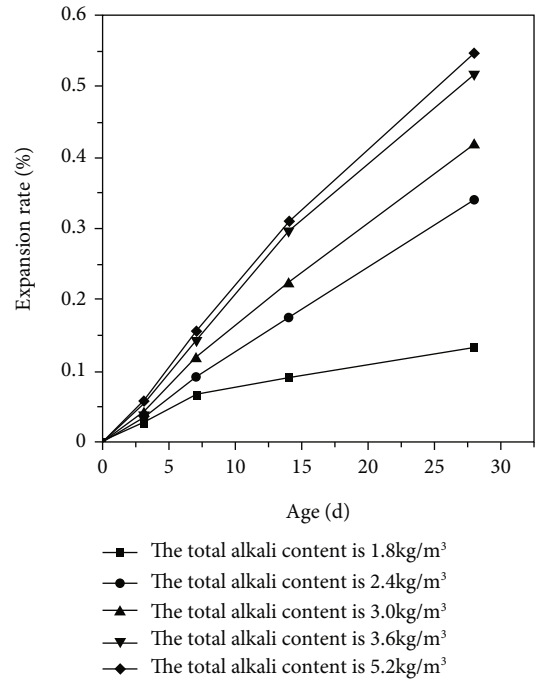

Figure 18: Graph of the effects of powdered coal ash mix on alkali-aggregate reaction.

4. Particularity and Design Scheme of Dam Concrete

4.1. Particularity of Dam Concrete. From the perspective of alkali-aggregate reaction, there are differences between dam concrete and ordinary concrete in the following aspects [26].

(1) The aggregate particle size is large. The aggregate particle size in dam concrete is large and accounts

Table 6: Horizontal and vertical displacement data.

Layout point number	Monitoring times	Maximum displacement (mm)			Average displacement (mm)		
		$\triangle X$	$\triangle Y$	$\triangle Z$	$\triangle X$	$\triangle Y$	$\triangle Z$
1	12	5	4	7	0	1	3
2	12	3	5	6	1	2	3
3	12	5	5	5	3	2	2
4	12	4	4	4	1	2	1
5	12	4	4	5	0	1	0
6	12	5	3	6	0	0	1
7	12	5	4	4	0	1	1
8	12	4	4	3	1	0	1
9	12	5	4	6	0	1	2
10	12	4	4	6	1	1	2
11	12	4	4	4	0	1	1
12	12	5	5	8	0	1	0
13	12	5	4	3	1	0	1

for a high proportion. Once alkali-aggregate reaction occurs, it will be more vulnerable to damage than ordinary concrete

(2) The strength of dam concrete is low. When the alkali-active aggregate inside the concrete reacts with the alkali happen alkali-aggregate reaction, the aggregate expands, and the cement stone will give the aggregate a force to inhibit the expansion of the aggregate. When the strength of cement stone is low, the tensile strength of cement stone will also be low, which means that the expansion force of aggregate that cement stone can bear is small, which further affects the concrete and makes the concrete prone to expansion cracking

(3) The amount of cementitious material is low. The reduction of cementitious materials will greatly reduce this inhibition and make the hardened cement stone bear greater tensile stress. From this point of view, compared with ordinary concrete engineering, dam concrete will be more vulnerable to damage once alkali-aggregate reaction occurs

(4) Wet conditions. As mentioned in the previous chapters, sufficient water is one of the necessary conditions for alkali-aggregate reaction

(5) Concrete dams have a long service life. In general, alkali-aggregate reactions are a very slow process, usually using "years" as a unit to calculate the time experienced before and after the reaction, sometimes taking decades or even decades to be observed. Concrete dam has the characteristics of large investment, long construction period, and long service life, which provides a "perfect" development time for the occurrence of alkali-aggregate reaction [27, 28]

4.2. Design Scheme. Restricted by objective conditions, the aggregates around Longtanqing debris flow gully treatment project are mainly sandstone with potential alkali activity. If other aggregates far away from the project area are selected, the transportation cost of aggregates will be seriously increased, so sandstone has to be selected as the aggregate of concrete. According to the conditions of alkali-aggregate reaction and the analysis of the inhibitory effect of coal ash on the reaction, two engineering measures are adopted for the dam in the study area: adding 35% class I class F coal ash and reducing the total alkali content of concrete [29–32].

The engineering can reduce the strength of alkali-aggregate reaction of dam concrete by using the method of high-mixed coal ash. Coal ash can adsorb alkali metal ions in concrete and reduce the effective alkali content of concrete. Coal ash react with calcium hydroxide in concrete to form high calcium gel and reduce the expansion rate of concrete. The dispersion of active silica particles in coal ash into concrete can disperse the local expansion force to the whole and reduce the damage of concrete. Coal ash can not only inhibit the damage of alkali-aggregate reaction but also reduce the hydration heat temperature rise of concrete and increase the tensile properties of concrete.

4.3. Experimental Verification. Class I class F coal ash, jade bead P.O42.5 cement and aggregate used in actual engineering are used to prepare experimental specimens according to the actual water binder ratio (0.56) and aggregate particle size of concrete. Refer to chapter III for specific operation steps.

In order to experiment the inhibition effect of coal ash on alkali-aggregate reaction, grade I coal ash with different content was used for experiment. The experimental results in Figure 17 show that when the content of grade I coal ash is 20%, 30%, and 35%, the 14-day expansion rate of concrete is reduced by 72.83%, 84.77%, and 90.12%, respectively, and the 28-day expansion rate is reduced by 79.61%, 87.20%, and 91.75%, respectively. This shows that the expansion rate of concrete decreases with the increase of coal

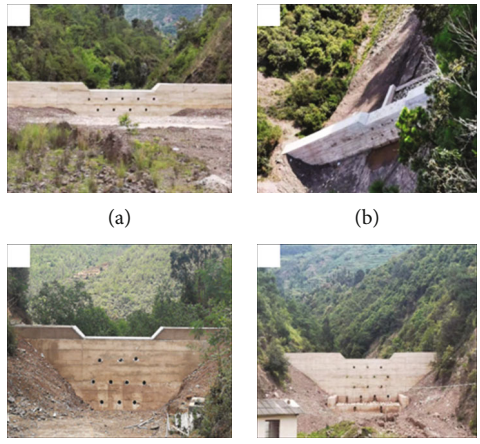

(a) (b) (c) (d)

Figure 19: Current situation of dam.

ash content. When the content of coal ash is 35%, it can effectively inhibit the expansion caused by alkali-aggregate reaction of concrete.

The experimental results of controlling the influence of total alkali content of concrete on concrete expansion deformation are shown in Figure 18. The experimental results show that the expansion rate of concrete increases significantly with the increase of total alkali content. Reduce the total alkali content of concrete from 5.2 kg/m^3 to 1.8 kg/m^3, and the concrete expansion rate will be reduced by 75.5%. It shows that in order to effectively inhibit the expansion damage caused by alkali-aggregate reaction, the alkali content of concrete should be reduced and selected the total alkali content of concrete 1.8 kg/m^3.

The experimental results show that the above two engineering measures can effectively inhibit the expansion deformation of aggregate in dam concrete and improve the service life of dam concrete.

4.4. Analysis and Verification of Horizontal and Vertical Displacement Data of Dam. A total of 13 monitoring points are arranged for this monitoring work, and the monitoring frequency is 1 month/time. From the completion of dam construction in March 2020 to the first ten days of March 2021, independent monitoring is carried out every month from the first to the tenth, and the monitoring accuracy meets the specification requirements. The statistical analysis of monitoring results is as (Table 6) follows.

It can be seen from the above table that the data of the dam is basically stable during the monitoring period of one year, and the average displacement is between 0 mm and 3 mm, indicating that there is no obvious deformation of the dam concrete. It further shows that the above two engineering measures can effectively inhibit the alkali-aggregate reaction of the dam concrete and improve the service life of the concrete.

4.5. Appearance Verification. The external manifestations of alkali-aggregate reactions in concrete are: a large number of "map shape" or "netted" cracks appear on the concrete surface. White colloidal substances often flow out of the cracks (except alkali carbonate reaction) and accumulate on the crack surface to form white sediments. After the completion of the dam after a long period of monitoring, the surface of the dam body intact, no "map shape" or "netted" cracks, nor see the appearance of white matter, indicating that the dam did not occur alkali-aggregate reaction in Figure 19, the above two engineering measures can effectively inhibit the dam concrete alkali-aggregate reaction, improve the service life of concrete.

5. Conclusion

In this paper, the failure mechanism of alkali-aggregate reaction is systematically analyzed, the experimental method of inhibiting alkali-aggregate reaction with coal ash is proposed, and the experimental research is carried out. The experimental results are fitted by MATLAB software, and the law and mechanism of inhibiting alkali-aggregate reaction with coal ash are obtained. Finally, the particularity of dam concrete is studied, and the design scheme is put forward according to the actual situation.

(1) The amount of admixtures, cement alkali content, and curing time can all have an impact on the alkali-aggregate reaction. The more fly ash is added, the smaller the expansion rate of the concrete specimen is, and the better the effect of fly ash in inhibiting the alkali-aggregate reaction; the greater the alkali content of the cement, the faster the concrete specimen's expansion rate. The faster the expansion rate of the concrete, the fiercer the degree of alkali-aggregate reaction of the concrete, and the greater the damage caused; the expansion rate of the concrete specimen increases with the increase of the curing age, showing a "convex" curve. The reaction rate of aggregate reaction decreases with time

(2) The content of fly ash and the expansion rate of concrete specimens are highly nonlinear and negatively

correlated. The higher the amount of fly ash, the lower the expansion rate of concrete specimens, the curing age, and the expansion rate of concrete specimens. It has a high degree of nonlinear positive correlation. The longer the curing period, the higher the expansion rate of the concrete specimen

(3) The optimum amount of fly ash appears at 30%-40%, and at this amount, fly ash has the strongest ability to inhibit alkali-aggregate reaction; when the content of fly ash is less than 20%, the fly ash ability to inhibit alkali aggregate reaction is weak

(4) From the perspective of economy, safety, and effectiveness, two engineering measures to inhibit the alkali-aggregate reaction are proposed: reduce the alkali content of concrete and use class I F fly ash with a high content of 35% as concrete admixtures. After multiple verifications, these two engineering measures have a good inhibitory effect on the alkali-aggregate reaction

Data Availability

The data used to support the findings of this study are included in the article.

Conflicts of Interest

The authors declare no conflicts of interest.

Authors' Contributions

The manuscript is approved by all authors for publication.

Acknowledgments

The authors acknowledge to the financial support from the Science and Technology Plan Project of Yunnan Provincial Department of Transportation of China under grant number Yunjiao Science and Education 2018-34 and Yunjiao Science and Education 2018-35. The authors would also like to acknowledge the State Key Laboratory of Hydraulics and Mountain River Engineering, College of Water Resource & Hydropower, Sichuan University.

References

[1] J. Pan, W. Wang, J. Wang, Y. Bai, and J. Wang, "Influence of coarse aggregate size on deterioration of concrete affected by alkali-aggregate reaction," *Construction and Building Materials*, vol. 329, p. 127228, 2022.

[2] P. Gao, *Study on Durability of Concrete Structure of Subway Engineering under High Altitude Saline Soil Environment in Northwest China*, Nanjing University of Aeronautics and Astronautics, 2018.

[3] M.-S. Tang, "About some theoretical problems on alkali-aggregate reaction," *Journal of the Chinese Ceramic Society*, pp. 365–373, 1990.

[4] M.-S. Tang, "Alkali silicic acid reaction and alkali carbonate reaction," *Strategic Study of CAE*, vol. 1, pp. 36–42, 2000.

[5] T. Ramlochan, M. Thomas, and K. A. Gruber, "The effect of metakaolin on alkali-silica reaction in concrete," *Cement and Concrete Research*, vol. 30, no. 3, pp. 339–344, 2000.

[6] F. Bektas, L. Turanli, and P. Monteiro, "Use of perlite powder to suppress the alkali-silica reaction," *Cement & Concrete Research*, vol. 35, no. 10, pp. 2014–2017, 2005.

[7] T. E. Stanton, O. J. Porter, L. C. Meder, and A. Nicol, "California experience with the expansion of concrete through reaction between cement and aggregate," *Journal Proceedings*, vol. 38, p. 38, 1942.

[8] S.-G. Zhou and Z. H. O. U. Xun-an, "ASR in high performance concrete structure (HPCS) and evaluation of suppression measures," *Journal of Northwestern Polytechnical University*, vol. 27, no. 1, pp. 137–143, 2009.

[9] X. X. Feng, Y. Jia, and C. G. Hu, "Effect of admixtures rich in aluminium on expansion due to alkali-silica reaction," *Applied Mechanics and Materials*, vol. 268, pp. 806–810, 2013.

[10] M. I. Khan, "HPC composites formulated to counteract early ASR expansion," *Journal of Materials in Civil Engineering*, vol. 25, no. 12, pp. 1951–1958, 2013.

[11] D. Harbec, A. Zidol, A. Tagnit-Hamou, and F. Gitzhofer, "Mechanical and durability properties of high performance glass fume concrete and mortars," *Construction and Building Materials*, vol. 134, pp. 142–156, 2017.

[12] Z.-Z. Xu, Y. Shen, D.-y. Lu et al., "Main parameters of a new experimental method for alkali activity of siliceous aggregates," *Journal of Nanjing University of Chemical Technology(Natural Science Edition)*, vol. 20, no. 2, pp. 2–8, 1998.

[13] H. Liu, *Study on Evaluation Method of Effectiveness of Fly Ash in Inhibiting ASR*, Nanjing Tech University, 2003.

[14] M. U. Salim and M. A. Mosaberpanah, "The mechanism of alkali-aggregate reaction in concrete/mortar and its mitigation by using geopolymer materials and mineral admixtures: a comprehensive review," *European Journal of Environmental and Civil Engineering*, pp. 1–41, 2021.

[15] X. Y. Zhuang, L. Chen, S. Komarneni et al., "Fly ash-based geopolymer: clean production, properties and applications," *Journal of Cleaner Production*, vol. 125, pp. 253–267, 2016.

[16] T. Hemalatha and A. Ramaswamy, "A review on fly ash characteristics - towards promoting high volume utilization in developing sustainable concrete," *Journal of Cleaner Production*, vol. 147, pp. 546–559, 2017.

[17] G. Xu and X. Shi, "Characteristics and applications of fly ash as a sustainable construction material: a state-of-the-art review," *Resources, Conservation and Recycling*, vol. 136, pp. 95–109, 2018.

[18] T. C. Esteves, R. Rajamma, D. Soares, A. S. Silva, V. M. Ferreira, and J. A. Labrincha, "Use of biomass fly ash for mitigation of alkali-silica reaction of cement mortars," *Construction and Building Materials*, vol. 26, no. 1, 2012.

[19] S. Kandasamy and M. H. Shehata, "The capacity of ternary blends containing slag and high-calcium fly ash to mitigate alkali silica reaction," *Cement and Concrete Composites*, vol. 49, pp. 92–99, 2014.

[20] K. A. Schumacher and J. H. Ideker, "New considerations in predicting mitigation of an alkali-silica reaction based on fly ash chemistry," *Journal of Materials in Civil Engineering*, vol. 27, no. 4, p. 04014144, 2015.

[21] H. Maraghechi, S. Salwocki, and F. Rajabipour, "Utilisation of alkali activated glass powder in binary mixtures with Portland

cement, slag, fly ash and hydrated lime," *Materials and Structures*, vol. 50, no. 1, 2017.

[22] R. D. Moser, A. R. Jayapalan, V. Y. Garas, and K. E. Kurtis, "Assessment of binary and ternary blends of metakaolin and class C fly ash for alkali-silica reaction mitigation in concrete," *Cement and Concrete Research*, vol. 40, no. 12, pp. 1664–1672, 2010.

[23] GB/T 50733-2011, *Technical Code for Prevention of Alkali-Aggregate Reaction in Concrete*, National Standard of the People's Republic of China, 2011.

[24] Z. Li, "Global sensitivity analysis of the static performance of concrete gravity dam from the viewpoint of structural health monitoring," *Archives of Computational Methods in Engineering*, vol. 28, no. 3, pp. 1611–1646, 2021.

[25] Z. M. Yaseen, A. M. S. Ameen, M. S. Aldlemy et al., "State-of-the art-powerhouse, dam structure, and turbine operation and vibrations," *Sustainability*, vol. 12, no. 4, p. 1676, 2020.

[26] M. Colombo and C. Comi, "Damage analyses of concrete dams subject to alkali-silica reaction," in *Conference on Italian Concrete Days*, Cham, 2016Springer.

[27] X. Huang, D. Zheng, M. Yang et al., "Displacement aging component-based stability analysis for the concrete dam," *Geomechanics & engineering*, vol. 14, no. 3, pp. 241–246, 2018.

[28] J. Y. Li, "Alkali aggregate reaction in dam concrete in China," *Hydroelectric Power*, vol. 31, no. 1, pp. 34–37, 2005.

[29] W. Zhong, J. Ouyang, D. Yang, X. Wang, Z. Guo, and K. Hu, "Effect of the in situ leaching solution of ion-absorbed rare earth on the mechanical behavior of basement rock," *Journal of Rock Mechanics and Geotechnical Engineering*, 2022.

[30] D. Pan, K. Hong, H. Fu, J. Zhou, N. Zhang, and G. Lu, "Influence characteristics and mechanism of fragmental size of broken coal mass on the injection regularity of silica sol grouting," *Construction and Building Materials*, vol. 269, p. 121251, 2021.

[31] D. Pan, K. Hong, H. Fu, J. Zhou, and N. Zhang, "Experimental study of the mechanism of grouting colloidal nano-silica in over-broken coal mass," *Quarterly Journal of Engineering Geology and Hydrogeology*, vol. 54, no. 4, 2021.

[32] H. Wu, G. Zhao, and S. Ma, "Failure behavior of horseshoe-shaped tunnel in hard rock under high stress: phenomenon and mechanisms," *Transactions of Nonferrous Metals Society of China*, vol. 32, no. 2, pp. 639–656, 2022.